A Low Positive Rate Attendant for Sickle Cell Anemia Screening in Health and Medicine

Avewe Bassene
Université Cheikh Anta Diop
Dakar, Senegal
avewe.bassene@ucad.edu.sn

Bamba Gueye
Université Cheikh Anta Diop
Dakar, Senegal
bamba.gueye@ucad.edu.sn

***Abstract*—African countries are facing a major public health problem due to hemogloblinopathies, which is the most common blood disorder in the world. In sub-Saharan Africa, 80% of the worldwide affected people (around 700 million) are living with sickle cell disease. Sickle cell anemia primarily affects children and teenagers and it unfortunately requires a life-long treatment from birth. Research reveals that in areas with no clinical follow-up, over 50% of children with sickle cell disease pass away before turning five years old. Health professionals assert that, depending on the patient's age and disease stage, early diagnosis and routine follow-up can prevent this scourge. However, standard and hand-operated diagnosis approaches, such as those used in Senegal and other sub-Saharan African nations, lack objective solutions and frequently require laborious decomposition operations that prone visual assessment errors. One of the most recent applications of AI is in medical decision-making, aiding doctors in diagnosis and treatment decisions. While interested in *CNN* learning model, ResNets, we propose an "Attendant of Screening for Sickle Cell Anemia" named (*ASSCA*) as a part of diagnosis decision-making. The *ASSCA* framework is able to accurately detect sickle cell disease and its development stage with a low false positive rate based on deep analysis of human blood smears images. In addition, based on knowledge of medical concerns, *ASSCA* gives better ways to measure disease assessment for rapid diagnosis decisions related to appropriate care. A key processing step is introduced to tackle classification challenges due to complex cell shapes, overlapped cells, and image color range. With a suitable optimizer (*SGD-M*), *ASSCA* gives an outstanding *mAP* measure of 98.81% with a low false positive rate.**

***Index Terms*—Deep learning, ResNets, Sickle cell anemia, Classification**

I. Introduction

Diagnosing and determining the staging of sickle cell anemia will help to recognize signs that can facilitate treatment and thus reduce morbi-mortality in most regions of Africa.

In Africa, in relation to most advanced healthcare facilities, treatment for Sickle Cell Anemia (*SCA*) is linked to regular medication prescribed by the doctor. However, the prescription is currently based on a subjective decision derived from sickled cells visual identification and counting operations which are based solely on the health expert's decisions. This tedious work is rated as inconsistent [1] and may lead to errors and an inappropriate diagnosis for the type of disease or even the stage of its development. Thus, in light of these limitations, several works attempt to enhance SCA diagnosis with the help of Artificial Intelligence (*IA*) tools. However, all of them have focused on improving the identification decision (decision-making capacity) of sickle cells at the expense of errors in that decision.

An AI model may decide whether or not a patient has sickle cell disease, but a model may also go wrong in this decision, which would be harmful and return to a misdiagnosis. Our issue will be an incorrect diagnosis decision due to the model's unsuitable diagnosis recommendation based on the stage of the disease. Section III will provide a more detailed depiction of that issue.

Microscopic inspection of blood smear samples from medical images can distinguish blood diseases in different parts of the human body. Deep learning ("DL") is an AI approach that has taken over existing traditional methods with its ability to process large amounts of data with outstanding levels of accuracy [2]. ResNets is a variant of convolutional neural networks. When it comes to classification, ResNets outperforms all other DL variants with its ability to extract the best features [3]. ResNets is able to extract at an acceptable time the characteristics that best correlate with the target variable. It also has the scarce ability to deal with degradation problems when saturation is reached throughout the model training process. To mitigate poor accuracy concerns in object detection, ResNets is combined with "YOLO version 5" to enhance SCA diagnosis by reducing errors in existing model decisions.

In this paper, we highlight a technical innovation in AI by joining the ResNets and YOLO architecture as a single hybrid proposal to accurately detect SCA. Our hybrid network simultaneously detects inspection points and classifies them in an accurate and reliable way. Furthermore, we show that a good combination of DL methods with medical professionals' knowledge has the potential to reduce costs and enhance productivity in health facilities, especially those of developing countries. Our main contributions are:

- We address a comprehensive learning framework for public health issues related to the diagnosis decision making on SCA;
- We propose an accurate framework, named *ASSCA*, that diagnoses SCA from blood smear images with a low type 1 error rate, ensuring better patient care and tackling manual diagnosis in local healthcare settings;

- We propose a new method to diagnose SCA based on the avoidance of sickling activities in blood [4] using a specific threshold of sickle cells rate. This new method can help save lives and improve patient care by automating the process with high precision;

The rest of this paper is organized as follows. Section II reviews related works. Section III depicts SCA shortcomings diagnosis problem and limits that lead to this proposal. The section IV exhibits our proposed DL-enabled object detection and classification approach that addresses existing concerns. Section V provides the experimental results and discussion. Finally, Section VI concludes our studies.

II. Related Works

Hajara et al. [5] propose an SCA detection framework based on AlexNet model. The Author's proposition first consists of Red Blood Cell (RBC) extraction based on their region of interest then, a CNN-based AlexNet model with transfer learning is used to classify these cells. The framework predicts cells based on a longitudinal study of patient cell shape with 90% of precision.

The authors in [6] propose a deep *CNN* model to classify sickle cells. Their proposal uses data augmentation approaches such as flipping, and rotating in the prepossessing step. Compared to DL-based models such as Resnet-50, Resnet-101, Visual Geometry Group (VGG-16, VGG-19), Inspection V3 outperforms with a accuracy of 91% in 0.001 learning rate.

In [7] authors use thresholding techniques to detect sickle cells. In this paper, morphological erosion and dilation preprocessing techniques are used to filter images to make their artifacts more visible. The outcome of this project is to highlight the gap between different parts of an image to distinguish normal and abnormal cell shapes. Binary image pixels are then inverted to keep only the abnormal cells visible.

Work in [8] aims to produce a classifier to identify SCA using multilayer perceptron (*MLP*). Based on a pre-processing step, 13 features are defined from image as the most relevant to diagnosis SCA. From the experimental result, *MLP* performs better than all machine learning algorithms with 98% of accuracy rate. MLP is one of the best ML algorithms when it comes to image classification. Can DL algorithms do better?

Using production-based AI tools, we propose an accurate model with low false alarm rates that deal with noise image quality, and effectively improve the accuracy of SCA detection. We refine ResNet-50 architecture as a simple feature extractor without its classifier component. Then we fine-tune the network output using YOLOv5 classifier layer to detect and count sickle cells. To the best of our knowledge, this is the first work that detects SCA and additionally provides insight into its prescriptions using this innovative AI mechanism. In contrast to work in literature, we use metrics as mean Average Precision (*mAP*) and false positives that are more suitable to evaluate object detection system performance.

III. Shortcomings of Existing Models

Sickle cell anemia is diagnosed by the presence of sickle cells in the blood. The early detection of SCA could help to remedy its disadvantage through specific treatment (i.e. insensitive to a specific antibiotic, blood transfusions, traditional plants to avoid sickling activities [4], analgesics, etc.).

Currently, intelligences are being developed using AI tools to compensate for errors in the manual diagnosis of SCA in local health facilities [5]–[8]. An AI model can determine whether a patient admits sickle cells or not. However, this decision is not uncontested as the intelligence used may be flawed in its decision. The decision-making problem can be described by the fact that intelligence can identify a malformed cell as not being one or can conversely state with great accuracy that a properly formed cell is deformed. The second case is more relevant to our study. Indeed, after SCA diagnostic studies such as [4] tries to prescribe treatment based on the percentage of sickle cells observed in a blood smear. The authors attempt to avoid the sickling activities according to the percentage of sickle cells in a blood sample over a field-of-view of the relative area of the smear. Thus, it is clear that a bad decision coming from AI can lead to erroneous prescriptions and hence life-threatening.

The motivation of this work is to bring more consistency with respect to the decisions made regarding the recognition of sickle cell. Thus, we propose a more efficient intelligence in terms of precision and especially in terms of error rate in the decision-making commonly known as false positives (*FPR*). This issue is tackled using a hybrid architecture combining two well-known algorithms ResNets and YOLOv5. YOLO [9] and ResNets [10]–[12] have proven their effectiveness in object recognition systems as well as powerful classification learners, respectively. In addition, delay and accuracy are two important criteria thanks to which ResNets is broadly approved in production. The proposed architecture and classification approach used in this survey are explained in the following sections.

IV. Materials and Methods

This section presents the architecture and data preprocessing methodologies adopted to improve learning from images. The proposed model architecture has two components: a feature extractor based on the ResNet-50 network and a classifier with YOLO "ObjectDetection" API. Since ResNets enables better learning, the classification technique we adopt implements ResNet-50 using Keras and readjust the output to the YOLO classifier layer for classification purposes. A detailed architecture is given in section IV-B.

Deep residual networks or ResNets [13] developed in 2016 seek to overcome two main problems of existing machine learning techniques; a long training time issue and a limited number of learning levels. Compared to other convolutional neural network architectures, ResNets performance does not decrease as the network architecture gets deeper. In addition, it avoids the vanishing gradient problem which greatly affects convolutional neural networks. ResNets is able to learn in deep

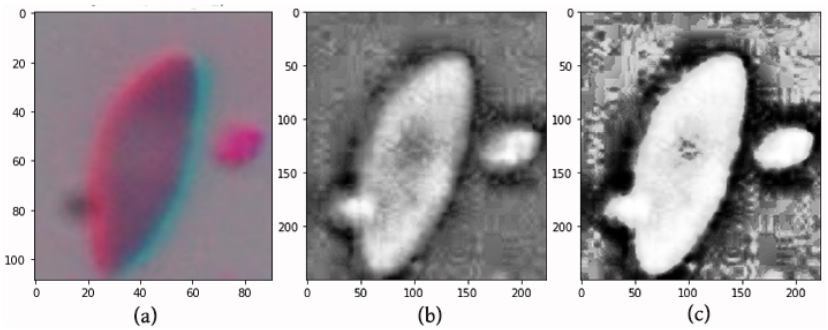

Fig. 1. Data-enhancing outcome : a) original image; b) grayscale image; (c) equalized image.

networks and it is shown that the model performs better in image classification than others *CNN* models [14]. ResNet-50 is a 50-layer convolutional neural network (48 convolutional layers, one MaxPool layer, and one average pool layer) that we use as a model training architecture in this experimental work. Training the network by using ResNets allows for better feature extraction on dataset images and thereby reduce the error rate (*FPR*) resulting in a disappeared gradient problem. ResNet has a significantly lower training error and can be generalized to validation data [13]

You only look once or YOLO [9] is a new approach to object detection. In its building mechanism, YOLO is not a classifier, nevertheless, we have re-purposed as such in our single-class classification problem. YOLO frame object recognition is a regression problem that spatially distinct bounding boxes and the object class probabilities directly from the full images. YOLO divides the image into a K x K grid where each grid predicts with probability Pr a delimitation box and confidence scores of these boxes to contain the object to be detected. A grid cell is responsible for detecting that object if only if the center of an object falls into that grid. To compute this center YOLO uses the well-known mathematical function *Intersection over Union* (IoU) that computes the symmetric difference of two sets of measurable geometric shapes, also known as the *disjunctive union* between shapes. The confidence score *Score* is evaluated using equation (1).

$$Score = Pr(object) * IoU \tag{1}$$

With its object detection methods and a customized enumeration function, YOLO provides us with a suited solution for sickle cell detection and counting from images. This has motivated the development of such a hybrid model. Our hybrid model that processes using dataset images with specific pre-processing is described in the next section.

A. Data Pre-processing

Our dataset is aggregated following two years of observation of sickle cell anemia cases. It was anonymously obtained from SCA smear specimens at the public hospital's hematology departments in Senegal. This dataset consists of samples of images obtained from sickle cell patients. Dataset consists of 727 blood smear full images with both normal and sickle cells. On random dataset images, cells are cropped then labeled with the help of at least two board-certified medical experts. The cells are dissociated into two folders; a folder named "abnormal" that contains 331 sickle cells and a folder with all other cells except for sickle cells called "normal". The normal folder consists of 396 samples that do not reflect sickle cell anemia according to diagnosticians panel. Using a multiple experts in the images labeling process help to improve model learning ability which firstly based on a human identification decision.

The image processing steps taken before training our model through the ResNets network are one of the key insights into our proposal. The pre-processing steps are two-fold: from the original image, we go for grayscaling, and from the grayscale image, we end to equalized image using *Adaptive histogram equalized* technique (AHET).

AHET is a data augmentation technique that generates more solid images, as well as all regions of the image. AHET helps to enhance image contrast by increasing discrepancy between the image's relative highs and lows in order to bring out subtle differences in shade. Indeed, YOLO bounding boxes are rectangular shape-based regression functions that determine the bounding boxes which correspond to rectangles highlighting the object in the image. The application of AHET on images afford enhancement on image details recognition while training the model. AHET, thereby brings more precision in YOLO shape recognition process. Since the detection of sickle cell (malformed cell) is particularly based on the cell shape (round or sickle form), equalized images learning from ResNets help to reduce error in both training and the final decision. The results can be striking, especially for grayscale images [15].

To sum up, the pre-processing steps involve applying a T transformation independently on each pixel of each original image in our dataset to get a better image. The outcome result is given in **Fig. 1**. The whole process is explained as follows.

For each image img with gray-level $\{i\}$ encoded on N (bits by pixel) level, the occurrence probability of a pixel with i_k level in img is formulated by equation (2).

$$P_i(i_k) = p(i = i_k) = \frac{n_k}{n}\ 0 \leq k < L \tag{2}$$

Where n_k is the number of occurrences of level i_k, n the total number of pixels in the image, and p_i the normalized histogram on $[0, 1]$.

The T transformation which for each pixel of i_k value of the original image associates a new value s_k denoted by $s_k = T(i_k)$ is formulated by (3). It consists of a final image representation commonly named *equalized histogram*.

$$T(i_k) = (L-1)\sum_{j=0}^{k} p_i(i_j) \tag{3}$$

Fig. 1 displays the outcomes of pre-processing images from the original dataset image to the final equalized image that we will use as input to train the model.

B. Hybrid Deep Learning with ResNets

After going through the pre-processing step, learning with the ResNets model is implemented. We design ResNet-50 architecture using the Tensorflow and Keras API. Each image in the post-preprocessing set is resized into 224x224, the dataset is split into 80% of training data and 20% for testing. **Fig. 2** provides the network architecture of our hybrid model along with an example of input pre-processed "abnormal" sample for the training phase.

The weights for ResNet-50 are initialized using *Stochastics Gradient Descent* (SGD) with standard momentum parameters. The *Momentum* can provide a big boost to SGD learning speed even with a little bit of change. It is shown to be beneficial for datasets whose samples share some features [16]. However, *Momentum* is therefore highly dependent on dataset structure and learning problems. Combined with SGD (i.e. *SGD-M*) *SGD-M* can accelerate training operation and memory improvements for model fine-tuning [17]. We perform the training steps in upward learning rates of 0.01, then 0.001 and 0.0001 by regularly minimizing loss parameters with *SGD-M*. The *SGD-M* tuning parameter is set to 0.934. The output of the training step is then flattened to build a YOLO classifier layer with a *dropout* value of 0.5.

In fact, *include_top* parameter is set to *False* to allow performing a YOLO classifier at the top of ResNet-50 architecture using the source input tensor. The model checkpoints are recorded for each learning rate using the Keras *callback* function. Thus, the performance evaluation is based on average precision and loss measures by epoch for different learning rates. The best learning rate is held for evaluation purposes.

C. Performance Evaluation

The evaluation criteria applied to evaluate the effectiveness of the proposed hybrid model are the (*mAP*) and the False Positive Rate (*FPR*). The model's ability to accurately identify sickle cells from an image and its confidence in making erroneous decisions are reflected by these metrics; i.e. high *mAP* and low *FPR* values. The *mAP* is selected as it includes the trade-off between precision and recall. It is also related to *FPR* and false negative measures. The equation (4) details the mathematical expression of these metrics.

$$\begin{aligned} Precision &= \frac{TP}{TP+FP} \\ FPR &= \frac{FP}{(FP+TN)} \end{aligned} \tag{4}$$

where TP is the number of true positives, TN is the number of true negatives, FP is the number of false positives.

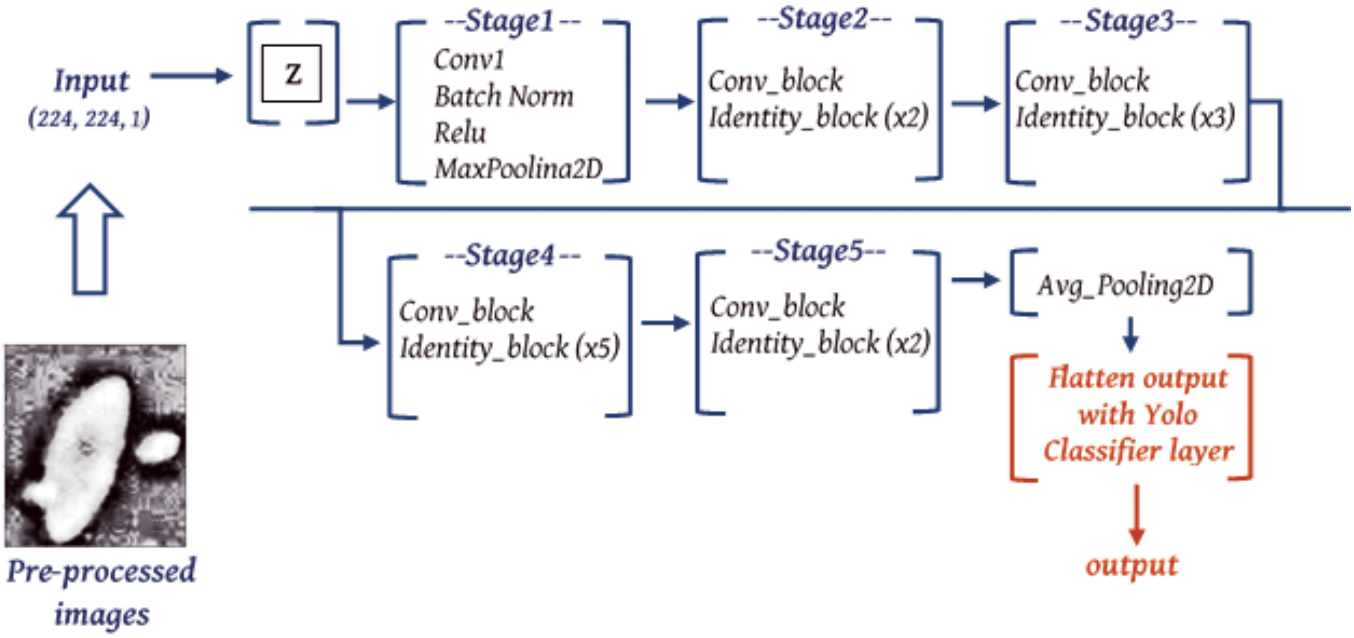

Fig. 2. Hybrid architecture design that ties ResNet-50 & YOLOv5

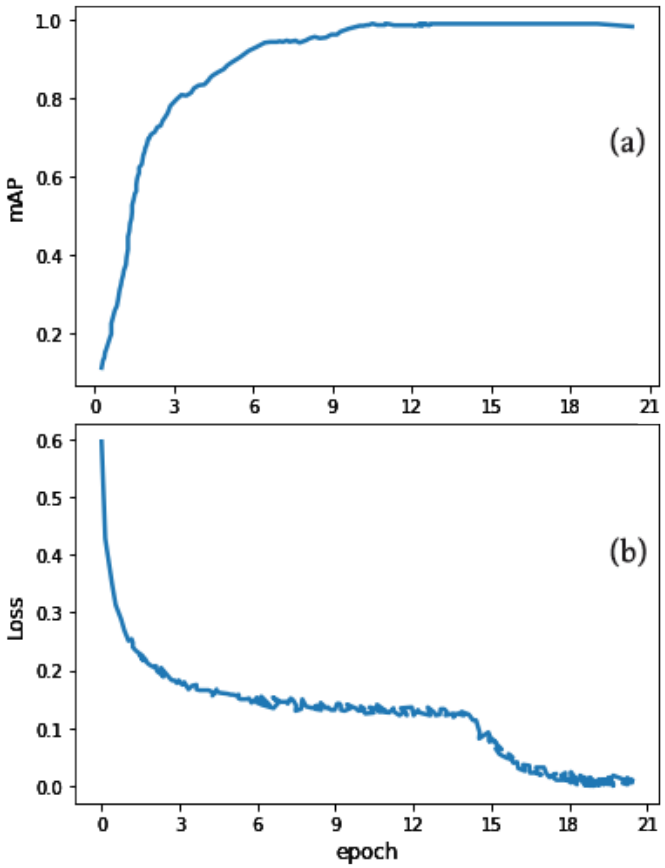

Fig. 3. Model performance outcome : a) Precision curve; b) error curve

V. Results and Discussion

To observe the model's ability to accurately identify sickle cells among the many other cells that make up human blood, *mAP* and loss change curves are depicted in **Fig. 3**. These values are the best overall recorded *mAP* and loss values per epoch with different learning rates. This observation were performed under 20 epochs.

In **Fig. 3** (a), it is worth noting that *mAP* gradually increases with the number of epochs. The higher overall *mAP* of 98.81% is recorded at the 14^{th} epoch, and the *mAP* value remains fairly stable thereafter. Adversely, **Fig. 3** (b) illustrates loss variation with epoch for the same learning rates. We can observe that the corresponding loss value linked to the better recorded *mAP* is 1.44%. However, the loss reached very low values from the 15^{th} epoch to end at a minimum of 0.31%. This unexpected drop is inadequate compared to the observations made on the *mAP* variation. We are currently unable to give an explanation for this observation. It may be linked to overfitting from the training network. However, this trend on the loss function in **Fig. 3** (b) announces the evaluation of the *FPR*.

The images used in this experimental test-bed were captured under an optical microscope with granularity per "field". The "field" index consists of the second digit of the microscope ocular. It allows us, from a magnification value of X100 to determine the observed diameter and then the targeted surface area of blood spread over a microscope slide. The value of this surface is required for the prescription and diagnosis of most cell-based diseases. This surface is associated with the number of cells in a "field" to give an exact diagnosis of SCA stage. For example, from local medical experts, determining 100 cells on a "field" helps when looking for the "leukocyte formula" or, the number of cells in the 200 "field" is used for bone marrow examination, etc.

From a magnification value of X100, we calculate that the images in the dataset are captured on around $0.25mm^2$ field-of-view across the blood smear area. Based on this result, we compared the diagnostic performance of our results with those of the authors in [1] in terms of *type 1* error ratio using a fixed learning rate of 10^{-3}. The **Fig. 4** reports the ROC curves that compared performance in SCA detection as opposed to work in [1] for the same patient slide images surface of $\sim 0.25mm^2$. In **Fig. 4** the x axis represents false positive rates, the y axis gives the true positive rate that is the proportion of cells that were correctly detected out of all sickle cells. The surface value is the same as the one on which our results are observed.

We can observe in **Fig. 4** that *ASSCA* provides better accurate prediction while classifying SCA from blood smear slides images than work in [1]. The trade-off between the two model's metrics (sensitivity and specificity) are close to the top-left corner with a better trend for *ASSCA* as depicted in **Fig. 4**. This means that with respect to classification, *ASSCA* performs better than the model proposed by Haan et al. [1] when images are captured in a specific microscopic parameters of $\sim 0.25\text{mm}^2$. The *ASSCA* performance results are particularly due to the data pre-processing step that deals well with typical YOLO-building mechanisms when processing object detection. The pre-processing step highlights the characteristics (shape and borders of the cell) learning ability of the ResNets network on which the YOLO algorithm bases its detection.

The pre-processing steps influence our testbed performance with better recognition of malformed cells. Indeed, with

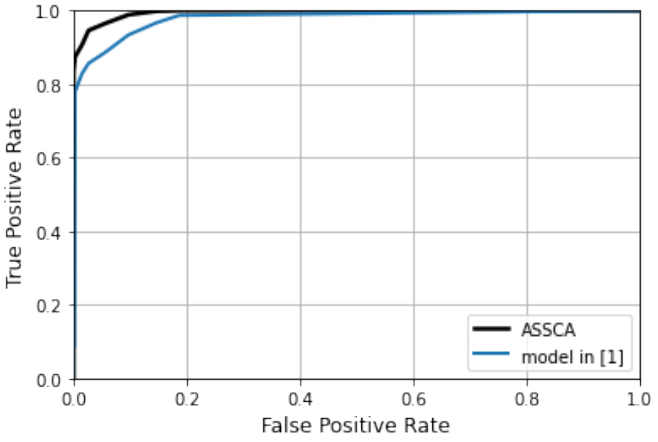

Fig. 4. Comparative ROC curves between ASSCA and model in [1] on a same blood smear surface of $\sim 0.25\text{mm}^2$:

thousands of human cells that are overlaid or blended with other neonate cells, the training process becomes arduous. In addition, various factors in images tend to overlap or scramble the edges of target cells, which are key element when identifying or detecting sickle cells.

Based on the implementation results of our hybrid method, we recommend the use of *ASSCA* to improve sensitive healthcare subjects as well as the detection of colorectal cancer [14], the classification of Lung Nodules [18], or leukocyte classification and recognition method [19]. The grounds of these recommendations is related to the works previously cited. The main focus of these papers is on precise diagnosis with low FPR and the knowledge of a targeted cell number in a delimited surface to provide better diagnosis. In addition, we suggest to the authors in the medical field to adopt *ASSCA* for safer diagnosis and the improvement of antisickling activities prescription which is jointly linked on the abnormal cells counting ability of proposed model. The proposed model can also be readjusted to determine the 'leukocyte formula' with it ability to determine the number red blood cells or platelets. In the health field, it additional has the potential to be a part of an examination process of the bone marrow.

The main limitation of *ASSCA* remains the threshold value of the percentage (over a field-of-view of $\sim 0.25 mm^2$) to diagnostic SCA. A poorly defined value can have a significant impact on Type 1 and Type 2 error rates. The percentage threshold has to be at least greater than 0.3% to avoid misclassification risks. Indeed, a low threshold rate (i.e. less than 0.3% of abnormal cells in a "field") could be a bad diagnosis since it has been shown that children without SCA admit on average 0.28% abnormal cells [20].

VI. CONCLUSION

In this paper, we aimed to link interdisciplinary academic researches that converge AI and clinical care to efficiently diagnosis SCA in its earliest state. This study combines medical professionals' knowledge and a production-based AI system to increase the effectiveness of SCA diagnosis and potential treatment based on proposals in healthcare [4]. Previous studies have investigated sickle cell detection to diagnose anemia. We address the type 1 error which is not emphasized in sensitive work related to blood diseases in general.

Our work based on a hybrid DL model automates SCA screening and diagnosis while considerably reducing the error related to decision-making. It is able to accurately predict SCA from blood smear images with high overall *mAP* of 98.81% and low FPR compared to literature.

The sudden drop observed in loss variation is not suited to learning indicators and must be further researched. In addition, we are aware that poor contrast tends to blur the sharpness of observations and model learning. We recommend our preprocessing step and we plan in the forthcoming works to expand on that point to reflect a standard in image taking process for better AI-based learning. Thus, answer some of the main challenges in AI clinical integration, standardization.

The threshold must be at least greater than 0.3% to avoid the risk of misclassification. This is one of the limitations of *ASSCA*. To be able to scientifically dissociate abnormal cells from regular cells in children's blood smear slides is a challenge that we set ourselves as an objective to reach in a new collaborations with medical experts.

REFERENCES

[1] K. de Haan et al., "Automated Screening of Sickle Cells using a Smartphone-Based Microscope and Deep Learning," CLEO. San Jose, CA, USA, pp. 1-2, May 2020.

[2] J. Deng, W. Dong, R. Socher, L. -J. Li, Kai Li and Li Fei-Fei,"ImageNet: A large-scale hierarchical image database", 2009 IEEE CCVPR. Miami, FL, USA, pp. 248-255, 2009.

[3] J. Liang, "Image classification based on RESNET," Journal of Physics: Conference Series. 1634. 2000.

[4] C. Sall, S. Ndoye, M. Dioum, I. Seck, R. Sylla, B. Faye, C. Thiam, M. Seck, P. Guéye, D. Fall, M.Fall, T. Dieye, "Phytochemical Screening, Evaluation of Antioxidant and Anti-sickling Activities of Two Polar Extracts of Combretum glutinosum Leaves,". Perr. ex DC. British Journal of Applied Science & Technology. Vol 19. pp. 1-11, 2017.

[5] A. Hajara, M. Razak, R. Sudirman, N.Ramli, "A deep learning AlexNet model for classification of red blood cells in sickle cell anemia," IAES IJ-AI. Vol 9. pp.221-228, June 2020.

[6] B. Sen, A. Ganesh, A. Bhan and S. Dixit, "Deep Learning based diagnosis of sickle cell anemia in human RBC," 2nd ICIEM, London, pp. 526-529, 2021.

[7] D. Saravanan, S. Rajasekaran, D.S. David, P. Hemalatha, U. Palani, "Detection of Sickle Cell Anemia from Microscopic Blood Images Using Different Local Adaptive Thresholding Techniques," Annals of RSCB, pp. 6549 –, Apr. 2021.

[8] S. Yeruva, M. Varalakshmi, B. Gowtham, Y. Chandana, P. Prasad, "Identification of Sickle Cell Anemia Using Deep Neural Networks," Emerging Science Journal. Vol 5. pp. 200-210, 2021.

[9] J. Redmon, S. Divvala, R. Girshick, A. Farhadi, "You Only Look Once: Unified, Real-Time Object Detection,". CoRR. 2015.

[10] J. Yuan, Y. Fan, X. Lv, C. Chen, D. Li, Y. Hong, Y. Wang, "Research on the practical classification and privacy protection of CT images of parotid tumors based on,". In Proceedings of the Journal of Physics: Conference Series. Volume 1576, p. 012040, UK, Jun. 2020.

[11] Z. Zheng, H. Zhang, X. Li, S. Liu, Y. Teng, "Resnet-based model for cancer detection,". In Proceedings of the IEEE ICCECE. Volume 2021, pp. 325–328, China, Jan. 2021.

[12] A. Deshpande, V. Estrela, P. Patavardhan, "The DCT-CNN-ResNet50 architecture to classify brain tumors with super-resolution, convolutional neural network, and the ResNet50," N.I. Vol. 1, no 4, pp. 100013, 2021.

[13] K. He,ZX,RS,SJ, "Deep residual learning for image recognition,". In in Proceedings of the IEEE CCVPR. pp. 770– 778, Jun. 2016.

[14] D. Sarwinda, R. Paradisa, A. Bustamam, P. Anggia, "Deep Learning in Image Classification using Residual Network (ResNet) Variants for Detection of Colorectal Cancer,". PCS. Vol. 179, pp. 423-431, Jan. 2021.

[15] A. Ryan, "Image Augmentation for Deep Learning using Keras and Histogram Equalization," https://bit.ly/3YsrnDZ (accessed Fev. 14, 2023)

[16] S. Jelassi,Y. Li, "Towards understanding how momentum improves generalization in deep learning," arXiv e-prints, Jul. 2022.

[17] M. E. Sander, P. Ablin, M. Blondel, G. Peyré, "Momentum residual neural networks," In ICML. pp. 9276-9287, 2021.

[18] P. Wu, X. Sun, Z. Zhao, H. Wang, S. Pan, B. Schuller, "Classification of Lung Nodules Based on Deep Residual Networks and Migration Learning,". Comput Intell Neurosci. Vol. 2020, pp. 1-10, Mar 2020.

[19] Y. C. Yang, W. Chen, "An Improved YOLO Leucocyte Classification and Recognition Method," ICITBSC. pp. 618-621, China, Mar. 2021.

[20] O. Alvarez, N. S. Montague, M. Marin, R. O'Brien, M. M. Rodriguez, "Quantification of sickle cells in the peripheral smear as a marker of disease severitym," Fetal Pediatr Pathol. Vol. 34, pp. 149–154, 2015.

[21] S. Busnatu, A. Niculescu, A. Bolocan, G. Petrescu, D. Păduraru, I. Năstasă, M. Lupușoru, M. Geantă, O. Andronic, A. Grumezescu, H. Martins. "Clinical Applications of Artificial Intelligence-An Updated Overview," J Clin Med. Vol. 11, pp. 2265, Apr. 2022.